CHAPTER 5. Results and discussion

5.1. Substrates characterization

5.1.1. Hydrated C_3S pastes

5.1.1.1. Mineral phases

XRD analysis is a tool that allows characterising the hydrated C_3S pasted manufactured (also referred to in the following as CSH for being its major compound and the only one containing CSH). In order to identify present phases it is necessary to turn to existing literature and previous works, as well as other complementary tools in order to know the pattern associated to each compound isolated in the resulting spectrum from the samples to be studied.

Feature spectrum of hydrated C_3S is shown in Figure 5.1. As C_3S is hydrated, its peaks loose intensity while portlandite ones keep on increasing. Non-hydrated C_3S presents a peak at about 33º. Considering values of 17º and 35º for 2θ angle from Figure 5.2, portlandite peaks are highly accused compared to the softer ones reached in the interval between 47º and 51º [Lin et al, 2003].

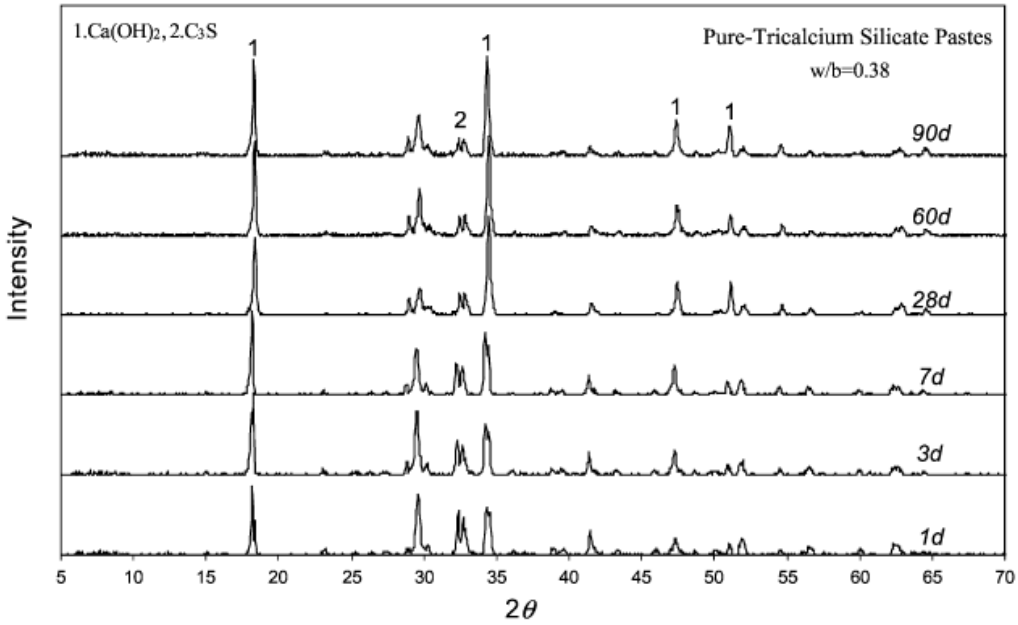

Figure 5.1. XRD pattern for hydrated C_3S samples [Lin et al, 2003].

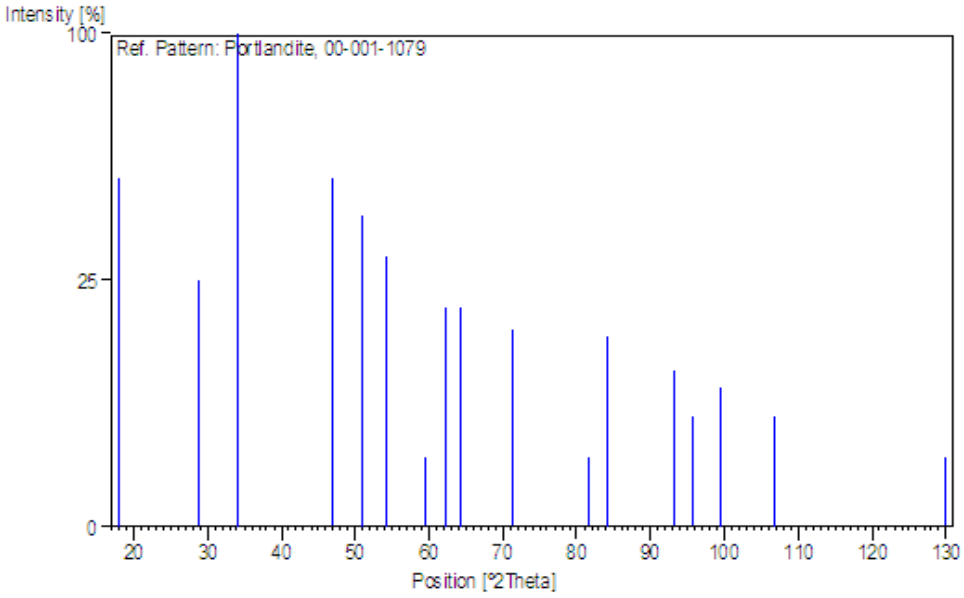

Figure 5.2. XRD pattern for portlandite [Pananalytical X'pert High Score software].

Therefore, it is also necessary to know $CaCO_3$ spectrum to indentify its contribution to the XRD spectrum resulting from C_3S samples. As seen in Figure 5.3, the major peak for $CaCO_3$ appears at 29º. Calcium carbonate peaks are expected to be of low intensity because its presence is associated to the carbonation of the sample; so, as exposition to atmospheric conditions has been carefully avoided, the amount of $CaCO_3$ shouldn't be remarkable. However, significant calcium carbonate peaks would mean that the manufacturing process followed in this study should be reconsidered or carried out in different controlled laboratory conditions.

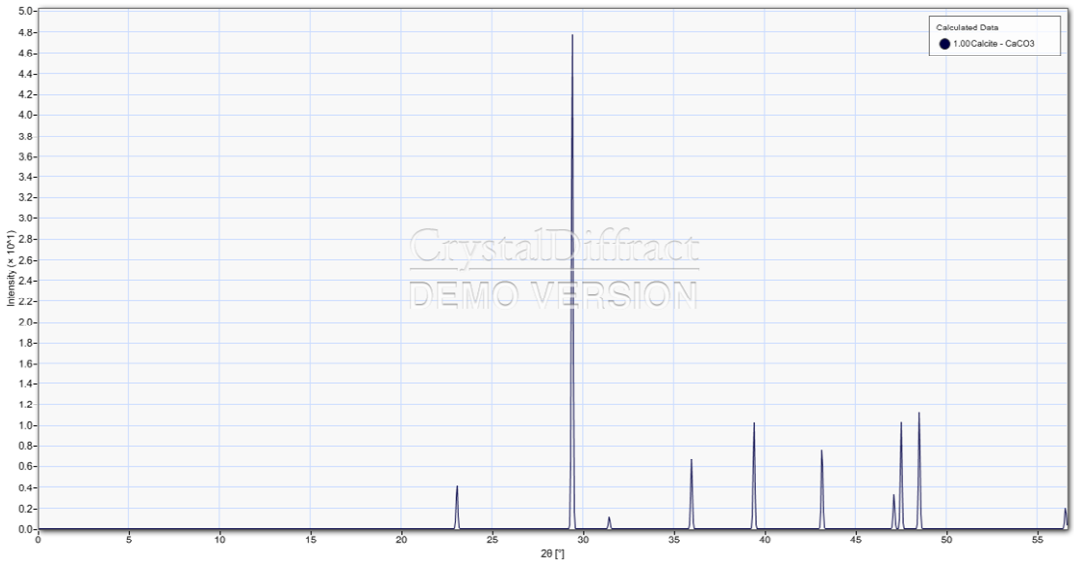

Figure 5.3. XRD pattern for $CaCO_3$. [CrystalDiffract™ software].

In this study, XRD analysis has been performed within a 2θ range between 5º and 50º because the main peaks expected to be found are covered by this interval of values. The XRD results are set in Figure 5.4, considering that legend coded numbers indicate the hydration time (days) of each sample followed by the number of the manufacture campaign (as already cited, samples has been manufactured in several stages, depending on the requirements of the research experiments).

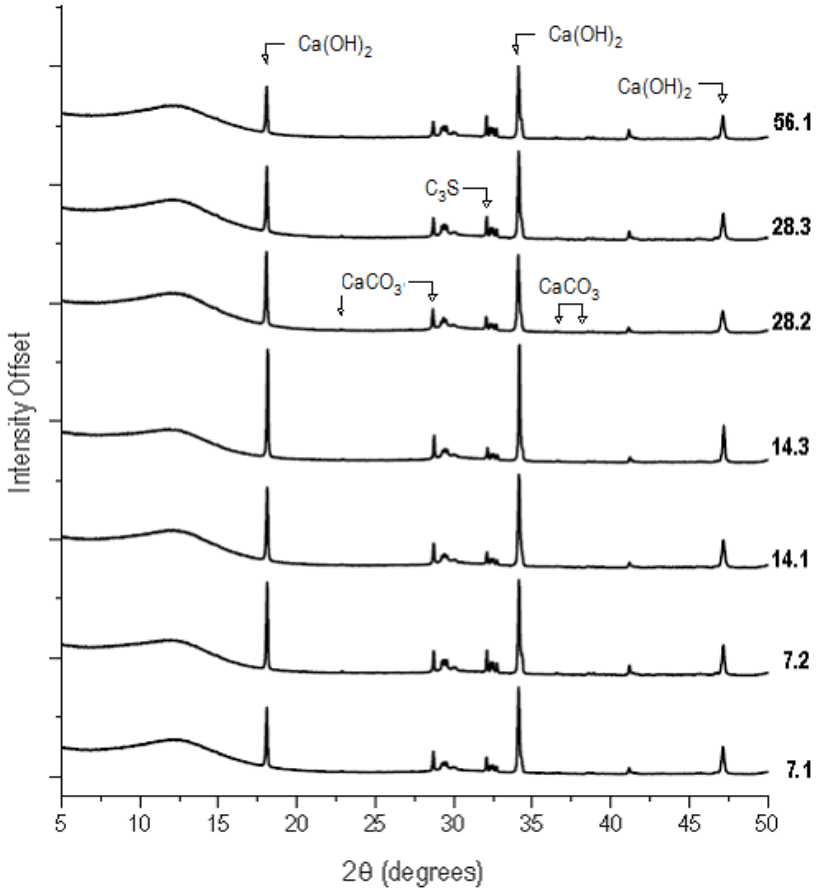

Figure 5.4. XRD spectrums for hydrated C_3S samples with identified peaks [OriginLab 8.0 software].

X-ray diffraction patterns were displaced for better visualization (with OriginLab 8.0 software) and it is noticed an increase on the porlandite peaks with the hydration exposure time, results expected according to the hydration mechanisms and products. It is seen that peaks associated to unhydrated C_3S grains are comparatively less intense than the portlandite ones. Although this is not a quantitative analysis it seems that a satisfactory hydration level has been achieved and the sample preparation process is acceptable, considering curing time as well as properly mixing water and C_3S.

There is also a $CaCO_3$ peak identified, indicating that the samples have undergone a carbonation process which must be taken into account. However, it is not notable in comparison to those for portlandite, considering that the samples have been isolated from the atmospheric environment.

5.1.1.2. Manufacture process reproducibility

One of the main objectives to achieve through TGA characterisation is confirming the reproducibility of the hydrated C_3S samples manufacturing process, i.e., that all the mixes have been performed the same way and consequently all the samples must have the same characteristics. To know it, samples from different mixes are compared through statistically. If the results are not much scattered (disperse), the following hypothesis would be accepted: accepting that manufacturing process as a mechanised process; therefore, for subsequent experiments using hydrated C_3S, all the samples (from mixes of different production data) will be grouped as a single amount of substrate, with no distinction.

Hydrated C_3S samples subjected to TGA are listed in Table 5.1. Except samples with a hydration time (cure) of 56 days, the rest belong to two different mixes.

Table 5.1. Outline of hydrated C_3S samples characterised by TGA.

Hydration time (days)	Nº samples	Mixes
7 days	4	1 and 2
14 days	4	1 and 3
28 days	10	2 and 3
56 days	3	1

Results for hydrated C_3S pastes are presented in Table 5.2, focusing on relative standard deviation values. On the one hand, standard deviation value of any variable provides information about how dispersed are the data collection from the average data. Ruling out systematic errors that can be attributed to equipments defects, the smaller dispersion the better approximation has the collected value as a real average; consequently, there will be less error committed by taking the average as estimator of the variable. On the other, relative standard deviation provides information about the importance or magnitude of this error associated to the estimated value. I.e., it would be possible to have standard deviation value which seems small (e.g. 0.5) but, if weighted on the average value (e.g. 0.75), it would become very important (66.7%).

Table 5.2. Portlandite amounts obtained in CSH characterisation.

Hydration time (days)		CH (%)*	$CaCO_3$ (%)**	CH' (%)	CH_T (%)
7	average	23	3.8	2.8	26
	st. dev.	1.5	0.71	0.53	0.94
	rel. st. dev (%)	6.2	19	19	3.6
14	average	23	4.4	3.2	27
	st. dev.	1.8	0,35	0.26	1.7
	rel. st. dev (%)	7.6	8.0	8.0	6.0
28	average	27	4.3	3.2	30
	st. dev.	1.6	0.51	0.36	1.6
	rel. st. dev (%)	5.8	11	11	5.4
56	average	25	5.3	3.9	29
	st. dev.	0.47	0.61	0.45	0.09
	rel. st. dev (%)	1.8	11	11	0.29

* ~400→500ºC / ** ~500→650ºC

Considering obtained values by looking at standard deviation, it's possible to state that manufacturing process is reproducible. Considering its relative deviation, previous hypothesis about reproducibility is regarded as valid because values are around 10%, which is the desirable maximum.

From now on, hypothesis cited above is accepted.

5.1.1.3. Portlandite content

Noting that drying the samples before starting the TGA essay is of utmost importance. It is recommended placing them in the oven at 60ºC for at least 8 h.

In Figure 5.4 are appreciated three curves (28.2.1, 28.2.2 and 28.3.1) with a different trend at lower temperature, corresponding to specimens without being previously dried. Hence, the initial slope is clearly much more pronounced than the remaining profiles, which remain much closer. As these three samples are not dried, so fast initial mass loss (pronounced slope) is related to humidity loss.

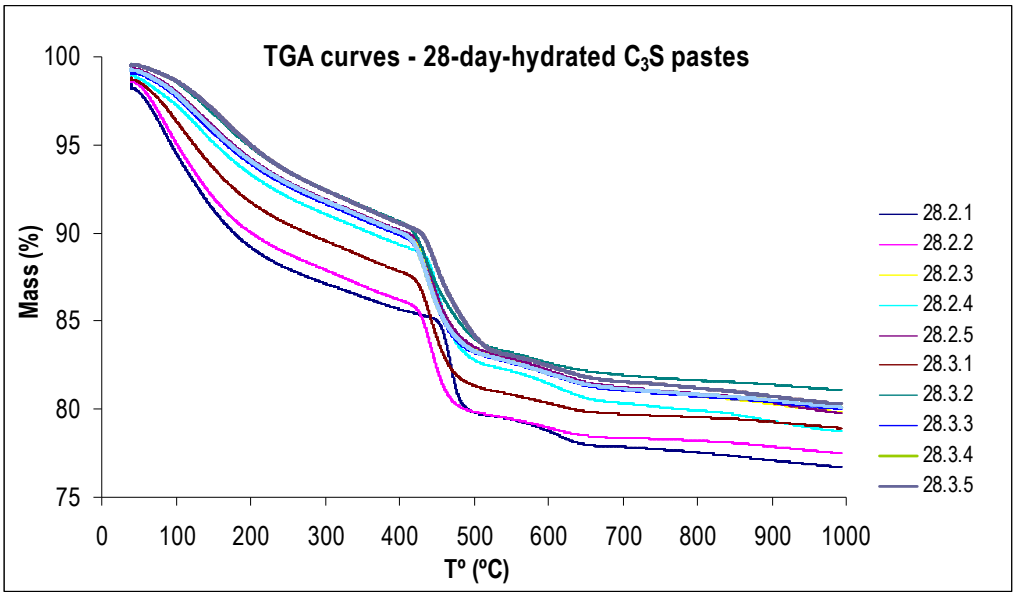

Figure 5.5. TGA curves for all the C_3S samples hydrated for 28 days (both dried and not dried samples).

By removing these data, graph curves get closer. Similarity between the data collected supports the previously accepted reproducibility in manufacturing process (mechanised).

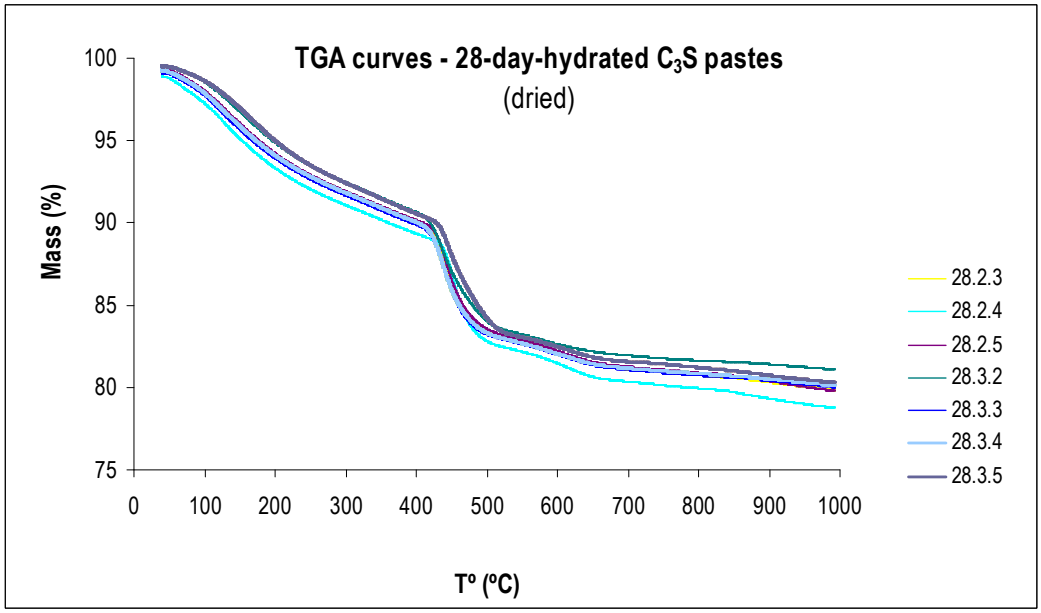

Figure 5.6. TGA curves for C_3S samples hydrated for 28 days, only the previously dried ones.

Table 5.3 shows the total portlandite percentages average (formed during hydration process) versus several hydration times (7, 14, 28 and 56 days). Values demonstrate how portlandite formation follows the expected pattern: its formation increases with hydration time until approximately 28 days. From this time on, its formation is stabilized, so the amount of portlandite in C_3S samples hydrated for 56 days are not increasing. In addition, total **portlandite formed values obtained in this study are close to the ones in previous works** [Chen et al, 2007].

Table 5.3. Portlandite amounts obtained in the CSH characterisation and amounts obtained in previous works.

	Hydration time (days)	% CH	% $CaCO_3$	% CH_T
Obtained values (average)	**7**	23	3.8	26
	14	23	4.4	27
	28	27	4.3	30
	56	25	5.3	29
Reference values Source: Chen et al, 2007	**28**	16.7	16.8	33.5

5.1.1.4. Ca/Si ratio

The main objective of SEM analysis is the calculation of Ca/Si ratio in CSH present in hydrated C_3S samples to be characterised. It is also useful for checking the proper hydration of C_3S grains through visual techniques as well as elemental maps provided by SEM.

It's necessary to emphasize that portlandite is not going to be identified as a present phase in the images because during the preparation of the sample (concretely during the polishing process to fit the samples format to the one required by SEM) deionised water was used as a lubricant, followed by aqueous diamond solutions. Hence, as portlandite is very sensitive to water, when getting in contact portlandite is dissolved. As a result, this phenomena causes that portlandite is not identified with SEM analysis, whereas CSH and unhydrated C_3S particles can be found.

In Figure 5.7, two different phases can be identified in the samples. According to SEM elemental analysis and comparing them with previous works [Mijno et al, 2004] it is possible to state that Spectrum 1, with Ca/Si=2.42, corresponds to a not hydrated C_3S grain; in contrast, the second phase found, which is darker and predominant (Spectrum 2), is CSH, supported by Ca/Si=1.38 obtained by elemental analysis (being reasonable as it is the main C_3S hydration product, together with portlandite). Both cited phases are also identified in Figure 5.8. Spectrums 1, 2 and 3 correspond to unhydrated C_3S grains, which are surrounded by a larger quantity of CSH phase identified by the remaining spectrums. The almost black parts of the images might be attributed to fissures produced along the hydration process as well as the grinding/polishing stage.

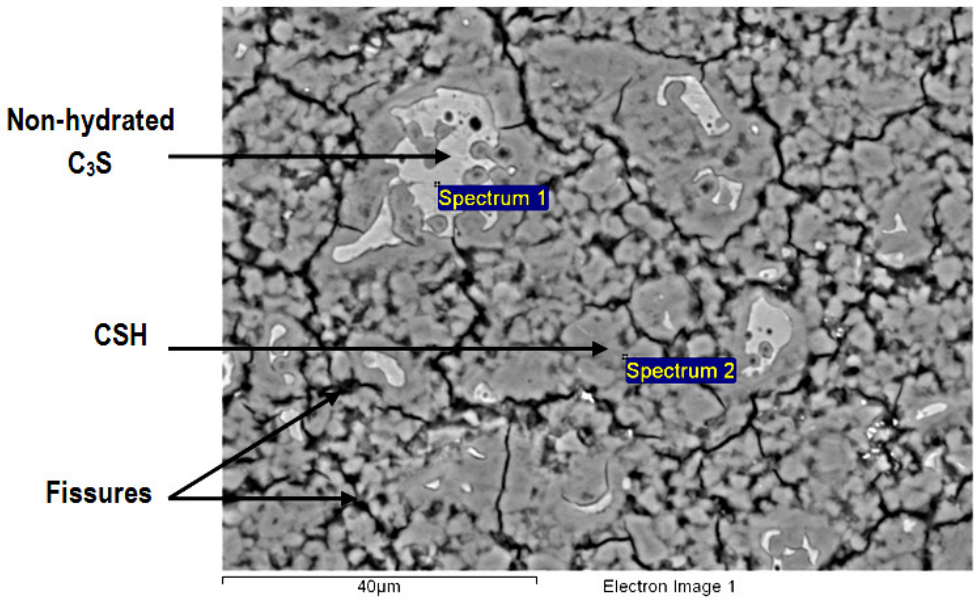

Figure 5.7. 28-day-hydration SEM image.

Resulting SEM images cover a large enough area of the sample to verify that actually, in proportion, the non-hydrated C_3S quantities are much lower than hydrated phases. Consequently, this fact confirms that the followed procedure for samples manufacturing is adequate. If non-hydrated C_3S quantities were the larger ones, the manufacturing technique would be undoubtedly rejected (so the above formulated hypothesis would not be accepted) because a good mixture between waster and the C_3S solid phase would not have been achieved.

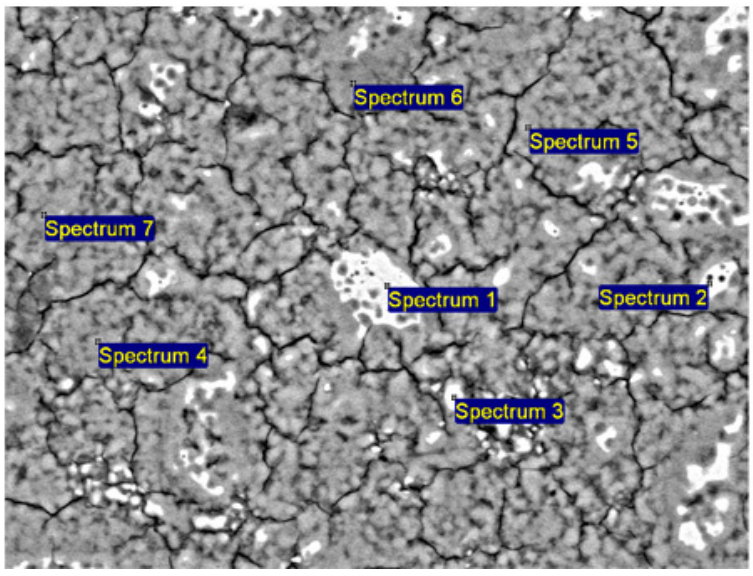

Figure 5.8. 28-day-hydration SEM image.

Considering images scale, it's possible to know the size of unhydrated grains from Figure 5.9: 24x32 µm (left) and 15x9 µm (right), meaning small surface area on the entire area imaged. Therefore, considering its small sizes and that represent just a little part of the whole sample, manufacture process in section 4.1 can be accepted.

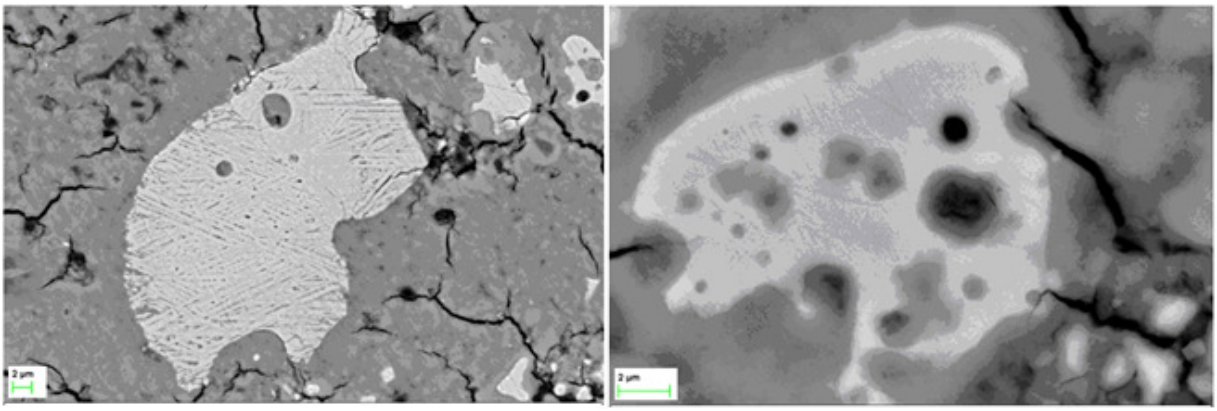

Figure 5.9. Unhydrated C_3S grains SEM images.

Considering all resulting elemental maps, the average value obtained for **Ca/Si ratio** based on 104 CSH data is **1.19**, and the average interval considering an 80% of confidence level is **[1.14-1.23]**. Normally, Ca/Si ratios for OPC are about 0.8-1.8 [Harris et al, 2002], and although the studied material in this study is not OPC, the Ca/Si ratio should be very similar because Portland, a part from C_3S, also includes oxides of several elements (e.g. aluminium or iron) which should not vary this ratio in CSH material.

5.1.2. Commercial portlandite

It must be checked that portlandite used for carrying out the experiments is in good conditions, meaning that it is low carbonated in order to be sure to attribute the whole results to portlandite behaviour. As shown in Figure 5.10, the TGA results for two samples are almost overlaid, leading to assume great substrate uniformity.

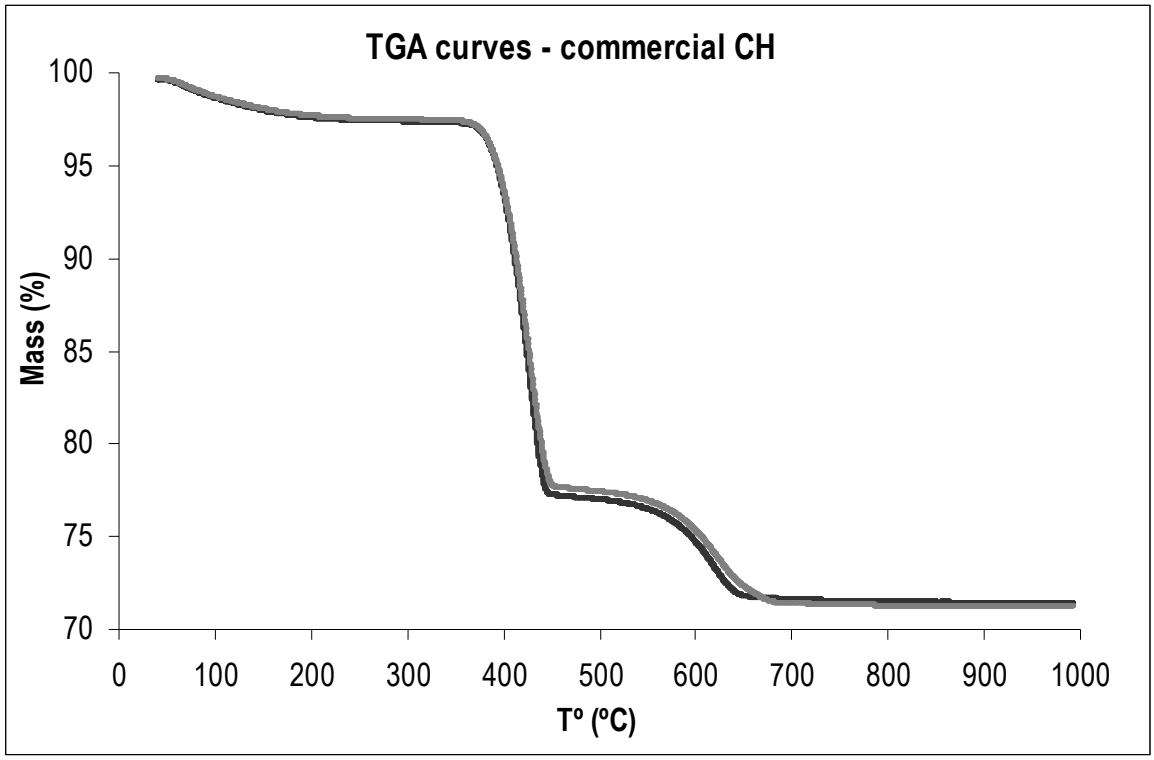

Figure 5.10. TGA curves for commercial CH samples.

It can be appreciated that the main content corresponds to portlandite as the most outstanding change of mass loss occurs at ~400-500ºC, corresponding to the its decomposition (dehydration) temperature. Nonetheless, it is followed by another mass loss assigned to the decomposition of carbonated mass for taking place at ~500-700ºC. In the image above, first mass loss due to sample humidity is not as highlighted as in CSH case.

According to section 4.2.1, portlandite contents (as a two samples average) are calculated for commercial portlandite. Despite $CaCO_3$ amount is more than 10%, as **portlandite is still the dominant compound** (~90%) it's possible to state that the input contaminants behaviour in the system will be related or explained through its interaction with portlandite more than calcium carbonate. Even though, it would be recommended performing the same experiment with also $CaCO_3$ as a substrate in order to know possible deviations in the output data due to $CaCO_3$ presence, which leads to portlandite carbonation.

Table 5.4. Total amount of portlandite obtained in the commercial CH characterisation

	CH (%)	$CaCO_3$ (%)	CH_T (%)
average	80	14	90
st. dev.	1.8	1.1	1.1
rel. st. dev (%)	2.3	7.6	1.2

5.1.3. *Insitu* portlandite

It must be guaranteed that CaO to be used in this experiment is neither hydrated nor carbonated. Therefore, in order to base the results in a pure substrate, CaO was heated up to 800ºC for 12 h in a mufla to ensure the absence of water molecules and also $CaCO_3$ (its decomposition takes place at ~500ºC → ~750ºC temperature interval). As already cited in section 3.3.3 (Table 3.2), from 750ºC there's a really small mass loss, considered minimal, so chemical reactions related to portlandite and calcium carbonate decomposition have completely finished; consequently, the only product which can be present in the resulting solid mass is CaO (calcined), according to Reaction 5.1:

$$CaCO_3\,(s) \rightarrow CaO\,(s) + CO_2\uparrow\,(g) \qquad \text{(Reaction 5.1)}$$

For this test, calcined CaO is mixed with water with L/S = 200. CaO is hydrated on water presence by Reaction 5.2:

$$CaO + H_2O \rightarrow Ca(OH)_2 \qquad \text{(Reaction 5.2)}$$

with no external energy input (ΔH_f = -985.2 KJ/mol) and room temperature. At several times, the mix is filtered in order to retain the solid mass which is later dried at 60ºC for more than 24 h.

Considering TGA results for the solid filtered mass from Figure 5.11, the most noteworthy mass differential while increasing temperature is the portlandite dehydration one, being followed by a less remarkable one related to calcium carbonate (originally from portlandite) decomposition. However, the more remarkable fact is the similarity between the three patterns despite its different hydration

times: they overlap and, as a result, is possible to determine that almost **the whole portlandite is formed throughout the first 60 minutes of hydration time**.

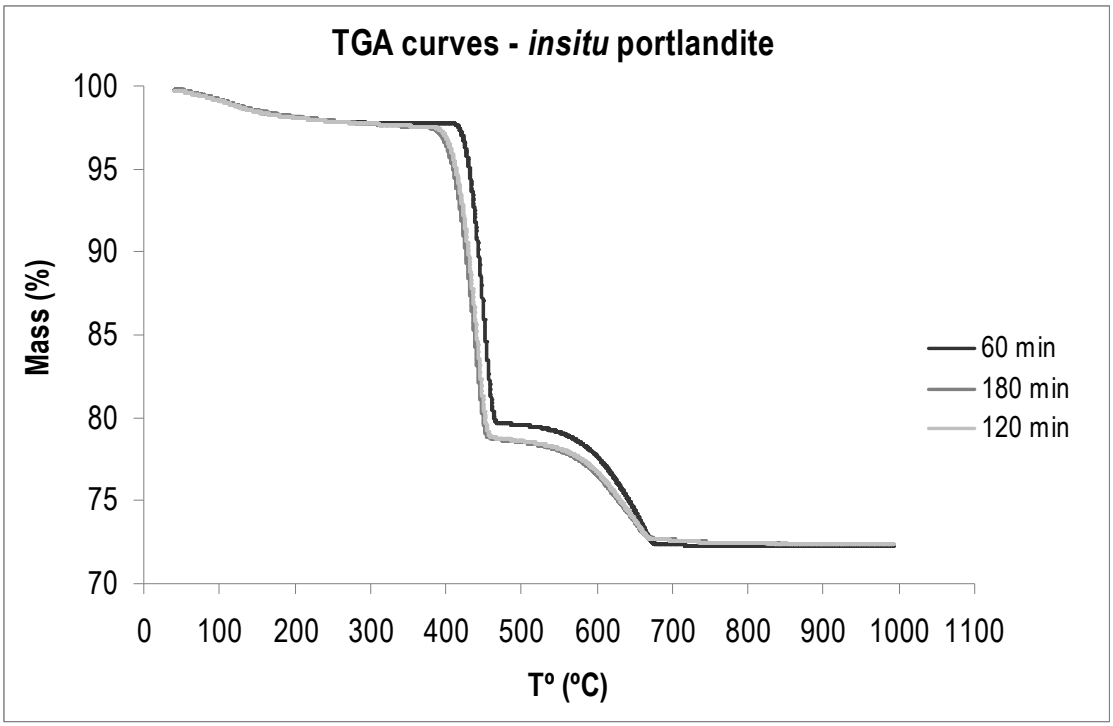

Figure 5.11. TGA curves for *insitu* CH samples of different hydration times (60, 120 and 180 minutes).

Table 5.5 shows portlandite contents for the three samples (including the carbonated and non carbonated quantities), calculated for *insitu* portlandite according to section 4.2.1. As can be appreciated, total portlandite amount for the first 60 minutes is slightly lower than later on, but it's so insignificant that it doesn't even change the average value, centred al 87%, together with a low standard deviation very insignificant.

Table 5.5. Total amount of portlandite obtained in the *insitu* CH (of different hydration times) characterisation.

		CH (%)	$CaCO_3$ (%)	CH_T (%)
Hydration time (min)	**60**	74	17	87
	120	78	14	88
	180	78	14	88
average		77	15	87
st. dev.		2.01	1.8	0.6
rel. st. dev (%)		2.6	12	0.88

Hence, comparing results obtained with commercial and *insitu* portlandite (in either of the times considered) and taking into consideration that standard deviations and relative ones are about 10% in both cases (which are acceptable), it's possible to conclude that, in terms of total portlandite amounts and composition, ***insitu* portlandite is absolutely comparable to commercial portlandite, being considered the same product.**

Table 5.6. Total portlandite amounts comparison (averages) between commercial and *insitu* CH.

	CH (%)	$CaCO_3$ (%)	CH_T (%)
***Insitu* CH**	77	15	**87**
Commercial CH	80	14	**90**

5.2. Vanadium retention experiments

5.2.1. Retention on commercial portlandite

The aim of this experiment is to evaluate portlandite role on vanadium retention from a solution, in order to know the chemical reactions between vanadium and water and, especially, to represent this metal evolution in the solution with time. For performing this experiment, commercial portlandite is used as substrate, previously characterized in section 5.1.2.

One of the main parameters to control while testing, which will determine the ionization degree in the system, is pH value, a determining factor in the case of adsorption [Weber, 1979]. Its evolution must be strictly controlled: if it keeps constant all over the experiment, changes in system's vanadium concentration can then be attributed to causes unrelated to pH changes.

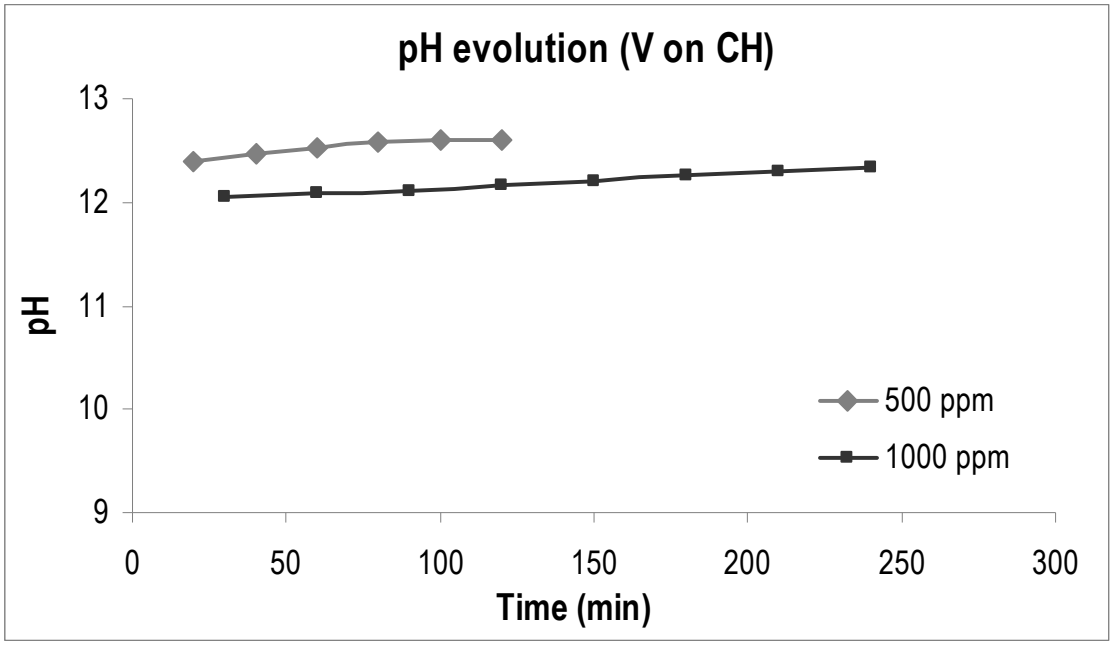

Figure 5.12. pH evolution for vanadium-portlandite system.

As desired to find, pH remains stable over the time, showing small increases lower than 0.3 units. Consequently, as pH keeps constant, vanadium elimination can not be explained by pH behaviour. It is remarkable that pH value obtained in all cases, finally, corresponds to the pH value for a portlandite saturated solution (pH≈12).

Vanadium elimination experiments show that different solution concentrations (500 and 1000 ppm of vanadium) lead to different equilibrium times. However, the complete vanadium removal from the

solution is achieved in both cases. It must be taken into account that the higher the pollutant concentration in the solution, the greater equilibrium time achieved and the greater adsorbed quantity, but not necessarily following a direct proportion [Weber, 1979].

Analyzing Figure 5.13, for a solution with a vanadium concentration of 500 ppm the equilibrium time is reached at 60 minutes, whereas it is reached at 120 minutes when considering 1000 ppm; so in the first case, the experiment lasts less time because the total vanadium elimination is achieved earlier. Having a higher concentration, the experiment is performed up to 240 minutes (to ensure the stabilization) knowing that the vanadium removal would be slower as well as conducting to a major equilibrium time.

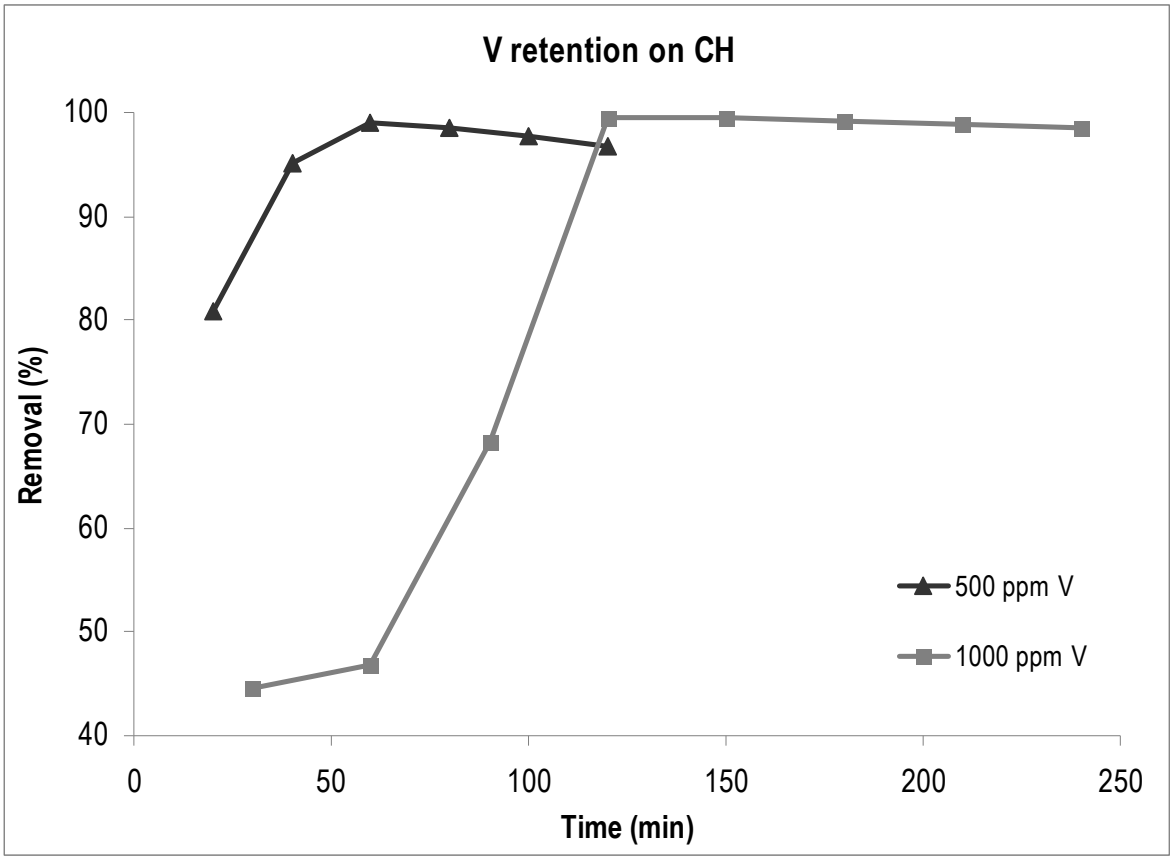

Figure 5.13. Removal percentage of vanadium from the solution (500 and 1000 ppm V) over time.

System mechanisms by which vanadium elimination occurs must be find out. Mention that removal percentages are calculated based on aliquots taken, i.e., results are based on supernate concentrations, in any case on the solid precipitated at the bottom of the container. Therefore, considering Figure 5.13, vanadium is no longer in solution: it moves to another phase of the test, which is basically the solid phase, i.e., **vanadium absence in solution** (supernate phase) **indicates a precipitation of the metal as solid phase.**

This hypothesis has to be confirmed and validated by theoric tools. Firstly, pourbaix diagram (explained in section 3.4.4) corresponding to the studied vanadium system must be considered in order to know its oxidation state and general expression. Through the eH-pH representation, it is confirmed that at very basic pH (pH≈12-12.7), vanadium acquires valence +5 and as HVO_4^{2-}.

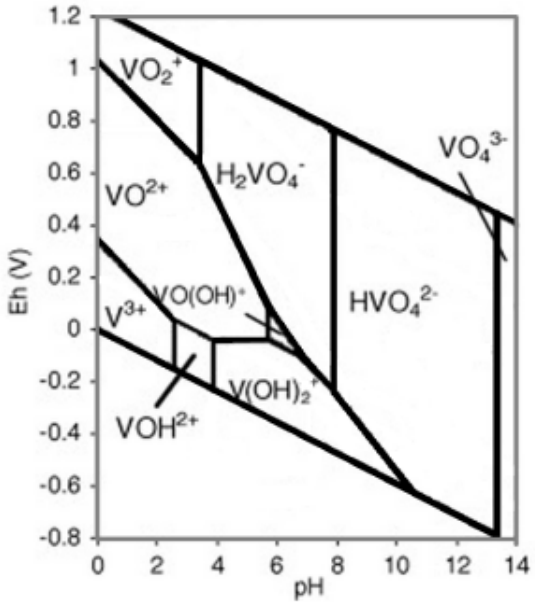

Figure 5.14. Main soluble species under the experimental conditions of this work
[Adapted from Cornelis et al, 2008].

Secondly, knowing that HVO_4^{2-} is vanadium predominant form and assuming Ca^{2+} ions presence due to portlandite dissolution with pure water, it's possible to model the experimental conditions (pH≈12.5, P≈1 atm, T°=24ºC) using PHREEQC software [Parkhurst and Appelo, 1999]. $Ca_3(VO_4)_2$ solubility-product constant at 25ºC is log K_{sp}=-17.97 [Allison et al, 1991], suggesting that such compound could be formed in the present experimental conditions (similar temperature). PHREEQC gives a saturation index (referred to in the following as SI), a numerical value useful for predicting HVO_4^{2-} stability in the water system, i.e., it indicates if the compound precipitates, dissolves or is in equilibrium, depending on:

- SI > 0, the compound precipitates because of the system's supersaturation;
- SI = 0, system is saturated (in equilibrium) with the compound;
- SI < 0, system is unsaturated and solid phase tends to be dissolved.

PHREEQC models a SI=2.53 (>0) for $Ca_3(VO_4)_2$, which confirms that vanadium precipitates as calcium vanadate, $Ca_3(VO_4)_2$, together with Ca^{2+} ions from portlandite dissolution.

Results obtained in vanadium retention experiments with portlandite are summarized as follows:

- **pH doesn't vary significantly**, so hydronium ions (H_3O^+) doesn't interfere in vanadium removal processes that take place in the solution.
- Vanadium is present as **hydrogenvanadate, HVO_4^{2-}**, in a very basic solution (pH≈12).
- Considering experimental conditions pH≈12.5, P≈1 atm and T°=24ºC, log K_{sp}=-17.97 [Allison et al, 1991] and SI=2.53 for $Ca_3(VO_4)_2$ obtained with PHREEQC, **vanadium elimination** from the solution **due to $Ca_3(VO_4)_2$ precipitation** is confirmed.

5.2.2. Coprecipitation with portlandite

The following experiment differs from the one performed in section 5.2.1 because the initial substrate is not portlandite but the reagent from which portlandite is formed, i.e., CaO (calcium oxide). Thus, processes to be studied are, on one side, substrate hydration in a vanadium solution and, on the other, pollutant's elimination. In order to analyse the first process, thermogravimetric analysis will be performed for hydration products characterisation. Contrary, oxyanions elimination is studied by ICP-OES technique of supernate removed.

Figure 5.15 represents TGA results, showing how portlandite amount formed in a vanadium solution varies for different times, in contrast to results obtained for CaO hydration with pure water (Figure 5.11). It also includes TGA pattern for portlandite formed with pure water (control) to appreciate at first sight that jumps are absolutely different in magnitude, which indicates a significant difference concerning portlandite amount in hydration products.

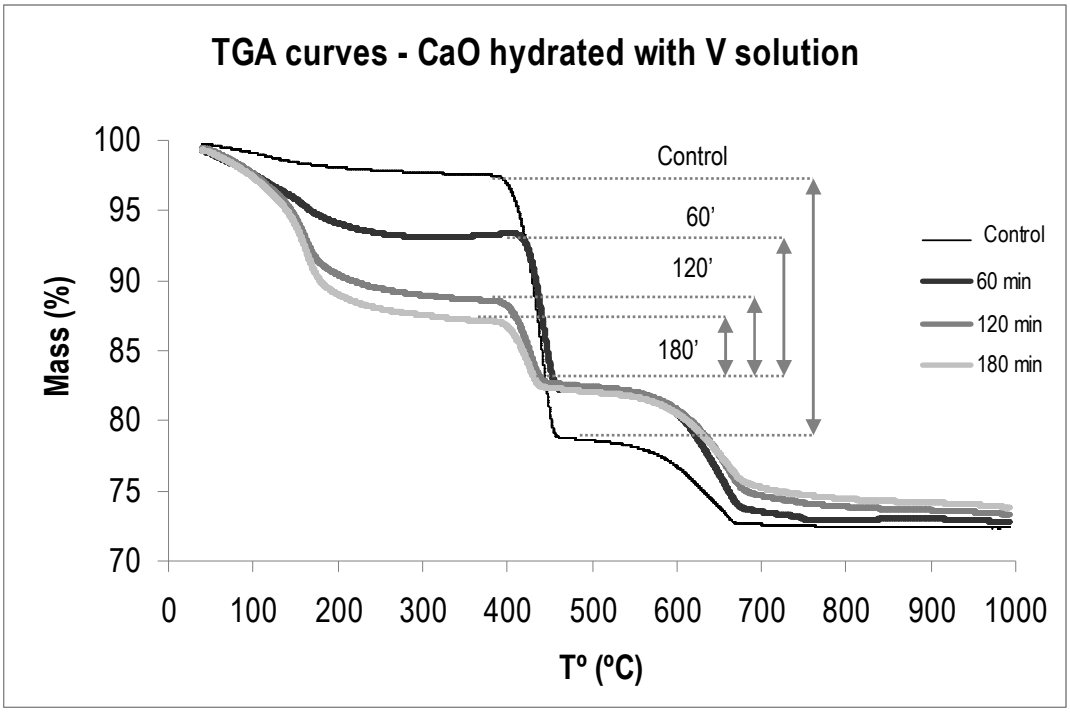

Figure 5.15. TGA curves for CaO hydrated with vanadium solution, highlighting the portlandite amounts difference for several time, including the characterisation of CaO hydrated with water (control sample).

According to section 4.2.1, Table 5.7 contains portlandite amounts calculated for the hydration products obtained.

Table 5.7. Total amount of portlandite obtained for hydrated CaO with V solution (at different times) characterisation.

Hydration time	% CH	% $CaCO_3$	% CH_T
60 min	46	20	59
120 min	25	18	38
180 min	19	16	30

As appreciated, portlandite formation decreases with time from 59% down to 30%. In view of section 5.1.3, portlandite formation doesn't decrease because the solution is saturated in calcium; therefore, solid-liquid interface reaches an equilibrium state. However, **vanadium addition in the solution alters this balance situation preventing the stabilization of portlandite formation with time**.

Based on the $CaCO_3$ calculation, it's possible to state that gradual portlandite decomposition is not translated to a greater amount of calcium carbonate formation because it also decreases with hydration time, although not so significantly.

Considering analogue trends for portlandite and carbonate formation over hydration time, it's necessary to raise the question of what is the fate of Ca^{2+} ions, thinking about two possible alternatives.

The first option to take into account is Ca^{2+} ions (presumably provided by portlandite dissolution) participation in a vanadate compound formation (as in commercial portlandite) like $Ca_3(VO_4)_2$. This hypothesis assumes an initial portlandite formation followed by its dissolution and, consequently, releasy of Ca^{2+} ions. Vanadium compounds have high melting points and would not cause any break in the TGA graphs obtained. Furthermore, when modelling the experiment with PHREEQC for *insitu* portlandite formation in a vanadium solution, SI>0 are obtained for these compounds: SI=1.42 for $Ca_2V_2O_7$ and SI=6.53 for $Ca_3(VO_4)_2$ (also expressed as $Ca_3V_2O_8$). PHREEQC also confirms numerically the precipitation of portlandite in the system through SI=3.94, meaning that portlandite doesn't reach the equilibrium, oppositely to the equilibrium achieved for commercial portlandite in vanadium solution (SI=0.0). Therefore, during CaO hydration in vanadium solution, both vanadium compounds and portlandite precipitate.

The second alternative, without being firmly justified, is that Ca^{2+} ions from CaO directly link to the formation of hydrous calcium vanadates, whose general formula is $xCaO{\cdot}yV_2O_5{\cdot}nH_2O$, where n sensitively depends on atmospheric humidity and varies from a minimum of 3 to a maximum of 9. Therefore, considering n value, there are two minerals: *hewettite* ($CaO{\cdot}3V_2O_5{\cdot}nH_2O$; $3<n\leq9$) or *metahewettite* ($CaO{\cdot}3V_2O_5{\cdot}3H_2O$) [Qurashi, 1961]. This variability in their mineralogical structure suggests that the 150ºC identified step may correspond to the dehydration of such compounds. At this temperature, mass loss for the unknown n-hydrated phase is increasing with hydration time, while portlandite jumps become smaller, and vice versa. However, further research is accurate in this field with the purpose of confirm the presence of such crystal. In addition, it is impossible to model the formation of hydrous calcium vanadates in the experiment because PHREEQC software uses equilibrium constants from a database that where neither hewettite nor similar compounds are included.

First argument based on vanadium compounds seems to be more justified, because although portlandite equilibrium is not reached, common vanadium compounds are formed to commercial portlandite test. Therefore, a priori, CaO behaviour in terms of vanadium retention would be really similar to that of portlandite.

Odd pH values don't help to explain this phenomenon as it doesn't remain constant over time and shows significant irregularities. As shown in Figure 5.16, pH evolution in vanadium solution doesn't

keep constant at all. There's a very accused low value, pH≈10 at ~90minutes, escaping from pH ranges obtained for the moment in this study. This irregularity could be interpreted as a sample contamination. However, considering pH value at 120 minutes, even at 60 minutes, they are both seldom lower, too, leading to an unusual profile that rarely seems fruit of an error.

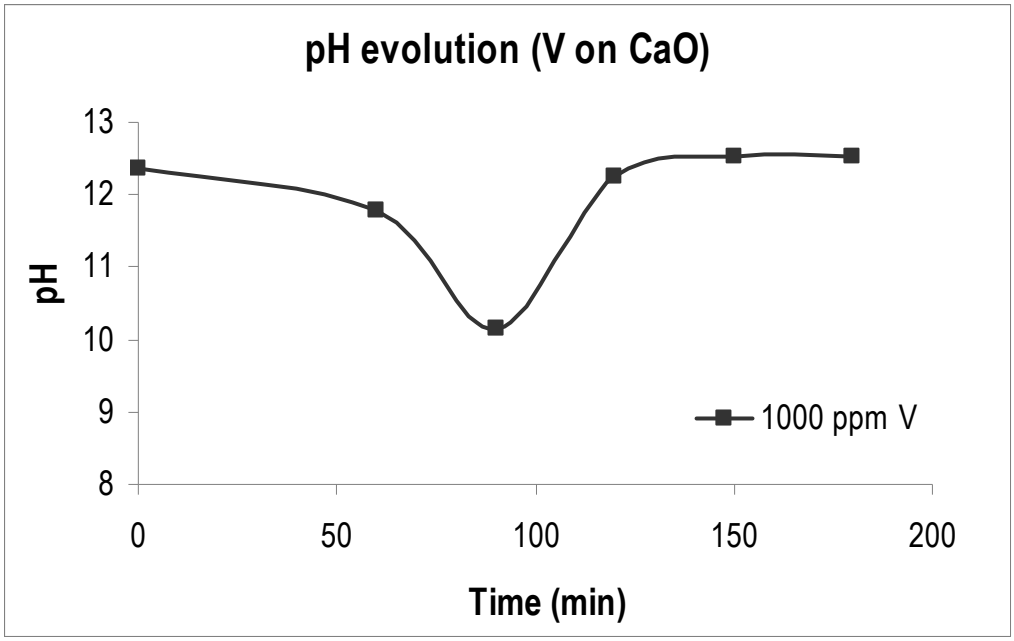

Figure 5.16. pH evolution for vanadium-hydrating CaO system.

Furthermore, TGA results don't include any evident variation likely to be connected with such pH irregularities. It would be possible to relate pH abrupt decreases to the formation-destruction of some species such as the vanadium compounds formation prior to that of hewettite. In addition, repeating the experiment is recommended with the aim of definitively ruling out the possibility of working with an altered sample.

Concerning Figure 5.17, it is questionable that both hydrating CaO and portlandite behave the same way in terms of vanadium retention. This suggestion previously formulated doesn't match completely with the obtained results. So, CaO retention behaviour is not the same to that of portlandite because they have different elimination rates. Even total elimination is achieved in both cases, CaO has a slower kinetics. This delay in metal retention might be associated to the simultaneous formation of portlandite and $Ca_3(VO_4)_2$. I.e., in the present experiment, not all the Ca^{2+} ions in the solution from CaO dissociation are only meant to generate $Ca_3(VO_4)_2$, but also to precipitate as portlandite.

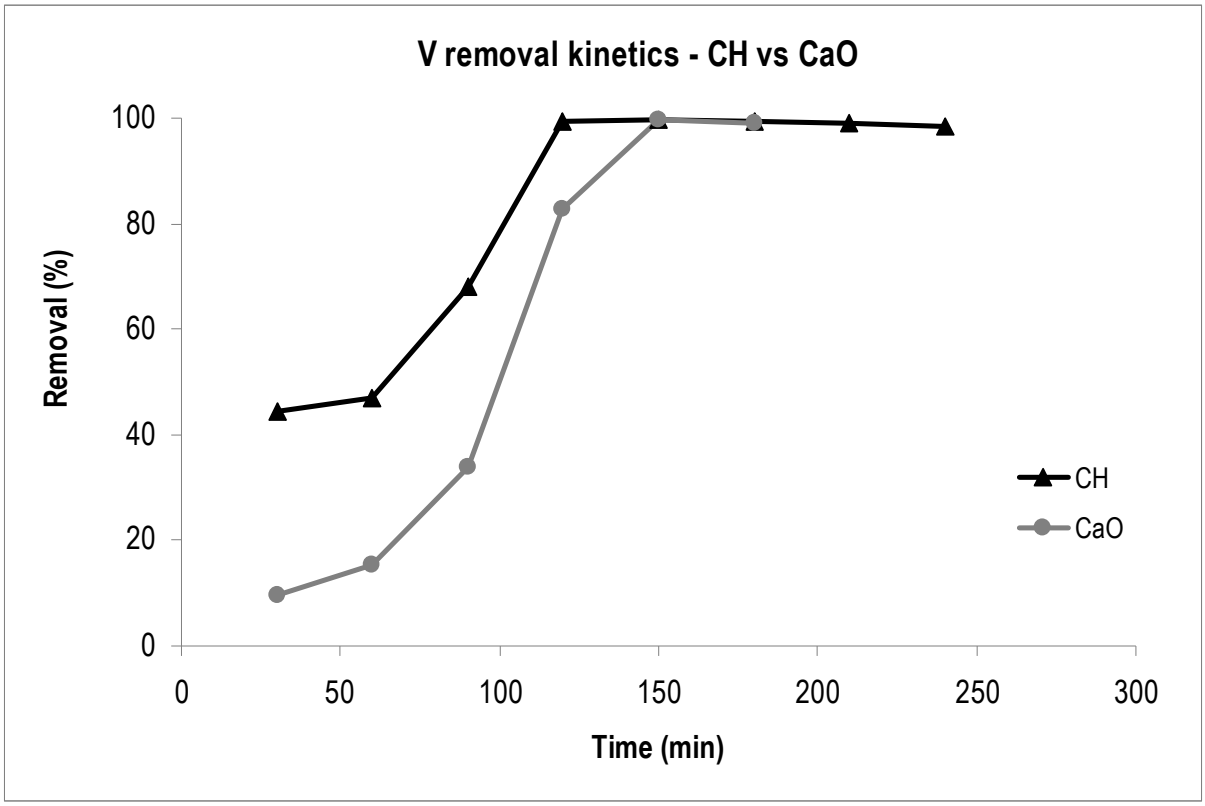

Figure 5.17. Vanadium elimination kinetics (for 1000 ppm V solution) on portlandite and hydrating CaO.

Results obtained in vanadium retention experiments with CaO are summarized as follows:

- Considering experimental conditions pH≈12.5, P≈1 atm and Tº=24ºC, log K_{sp}=-17.97 [Allison et al, 1991] and SI=6.53 for $Ca_3(VO_4)_2$ obtained with PHREEQC, **vanadium elimination** from the solution is related to **$Ca_3(VO_4)_2$** and **$Ca_2V_2O_7$ precipitation**.
- According to PHREEQC results**, portlandite is not in equilibrium with the solution** (SI=3.94).
- **Vanadium alters portlandite formation**; therefore, as portlandite is not stabilized, **total amount decreases** over hydration time.
- **TGA curves suggest the formation of a compound** that loses mass at ~150ºC, which is required to be further characterised with other techniques, as well as pH irregularities.

5.2.3. Retention on CSH

5.2.3.1 Analysis and justification of vanadium removal dynamics

As Figure 5.18 shows, the evolution of pH values remains almost constant, ranging from 12 to 12.6, without significant changes at different concentrations of the vanadium solution (500 and 1000 ppm). As in the case of CH, pH values correspond to the cement-based systems ones.

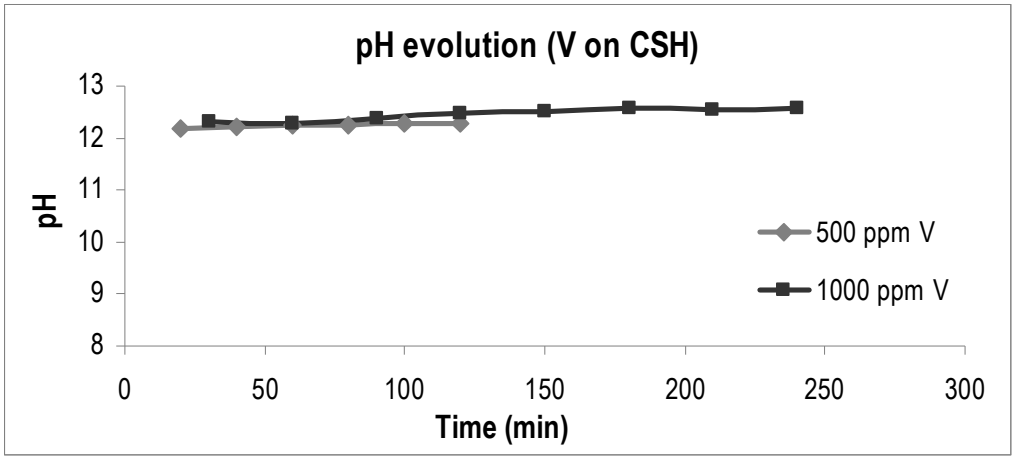

Figure 5.18. pH evolution for vanadium-CSH system.

Considering that pH values remain the same both in CH and CSH experiments, vanadium retention behaviour in both substrates should be, in principle, expected to be the same. However, as Figure 5.19 demonstrates, CH and CSH retain vanadium in different ways.

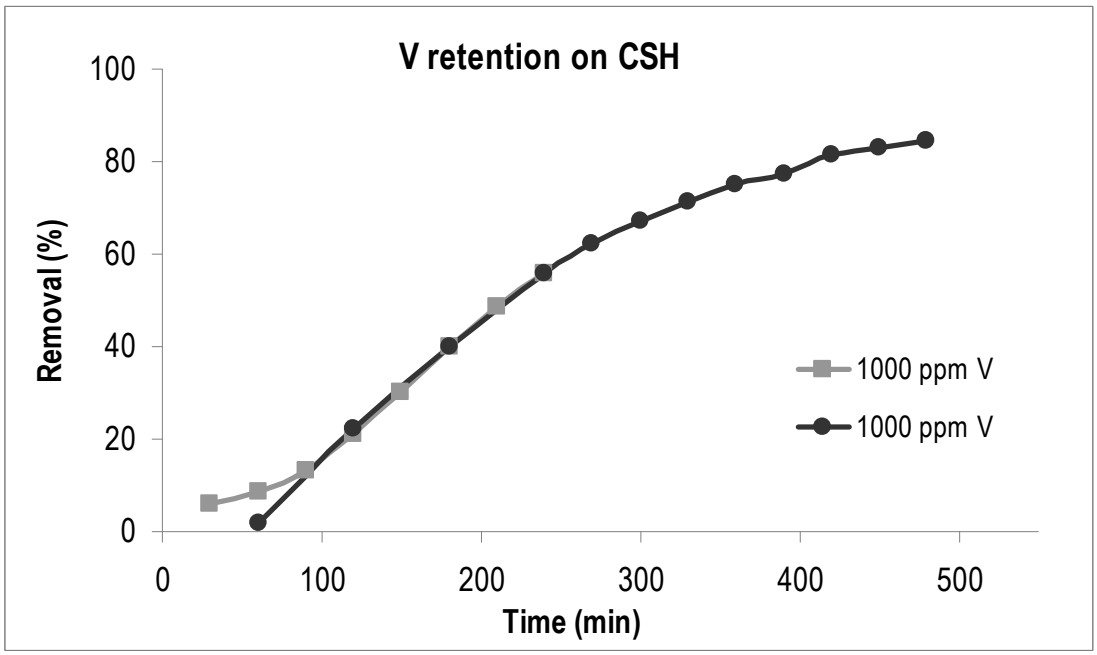

Figure 5.19. Removal percentage of vanadium from the solution over the time.

In the case of CH, the system equilibrium is reached faster at 120min and, afterwards, a precipitation mechanism of $Ca_3(VO_4)_2$ takes place, removing the whole HVO_4^{2-} oxyanions from the solution.

Opposed, in the case of CSH, the same trend is not observed: there's only a partial removal, without reaching the 100% of vanadium elimination. Presenting the results from the solution of 500 ppm of vanadium would be irrelevant because, as the case of commercial portlandite (section 5.2.1), results obtained with a 1000 ppm solution already include the trend followed with a solution of 500 ppm.

The reason why Figure 5.20 shows the evolution of two 1000 ppm systems is that, to start, the experiment performed at the beginning doesn't last enough to reach the equilibrium. But in both

1000ppm solutions, the removal of vanadium over the same follows an interesting trend. In the series up to 480min, having a great coincidence of values with the series up to 240min, is possible to deduce that the system is nearly arriving to the equilibrium due to a significantly decreased slope. Having different retention trends on two different substrates that have the same pH means that CSH plays a role that prevents 100% precipitation of vanadium as $Ca_3(VO_4)_2$.

In order to demonstrate and confirm the presence of CSH nanoparticles in suspension, it's possible to know how the Ca/Si ratio changes with the time analysing Ca and Si concentrations in the solution from extracted aliquots by ICP-OES.

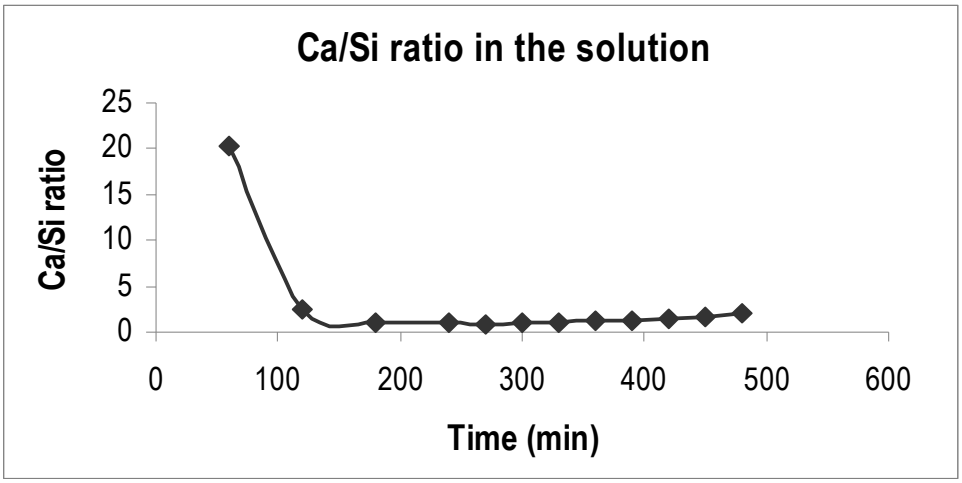

Figure 5.20. Ca/Si ratio evolution over time.

As perceived, Ca/Si ratio at 60 minutes is extremely high and it prevents a correct interpretation of the values obtained further on. Fast initial portlandite dissolution releases a high Ca^{2+} ions concentration in the solution, having an initial silicium absence ([Si]≈0). Both factors explain the isolated value obtained at 60 minutes. To better read the results, such point is skipped because, from then on, obtained results are reasonably comparable between them. Figure 5.21 displays the values adapted to the Ca/Si=1.7-1.8 usually found in literature for CSH [Bye, 1999].

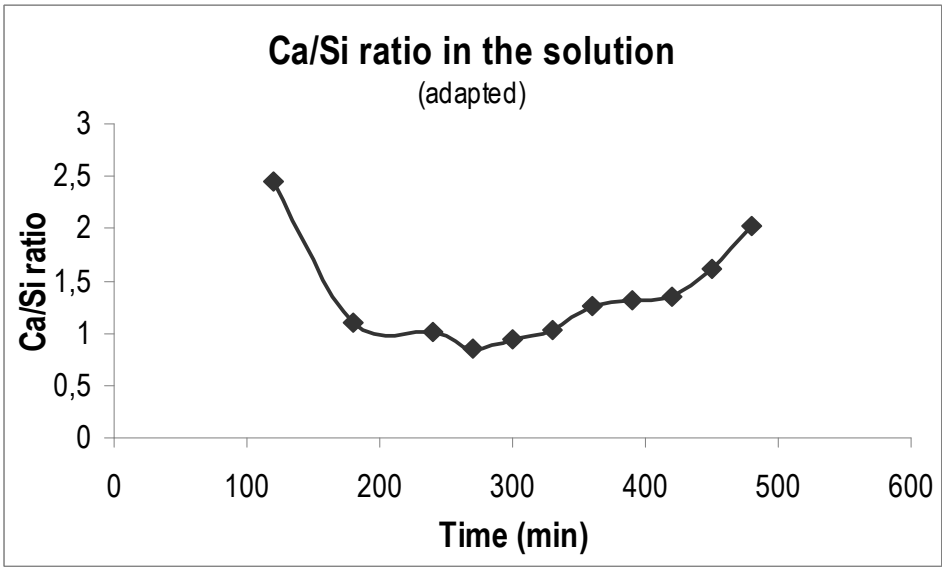

Figure 5.21. Ca/Si ratio evolution over time adapted to the usual Ca/Si ratios from literature.

As a conclusion, it's possible to confirm the presence of colloidal CSH nanoparticles (carrying oxyanions) because values obtained for Ca/Si ratio range from 0.8 to 2.5, including 1.19 value which is previously found for CSH samples by SEM characterisation (section 5.1.1.4).

It can be appreciated that there's no clear tendency in the behaviour of the Ca/Si rate in the solution in function of time. Figure 5.21 points out some factors which would be involved in explaining how Ca/Si ratio evolves:

- Initially, fast portlandite dissolution releases a high Ca^{2+} concentration in the solution, while having an initial silicium absence ($[Si^{4+}]\approx 0$). Both factors explain the isolation of 60 minutes Ca/Si ratio value, not considered owing its interference for results interpretation.
- After portlandite dissociation, CSH starts dissolving. CSH is less susceptible to pure water, so it dissolves later than portlandite. In this stage, Ca^{2+} ions are still released, and subsequently captured (either in colloidal CSH nanoparticles or precipitating as $Ca_3(VO_4)_2$), but Si^{4+} too. From this moment on both Ca^{2+} capture (while being released) and Si^{4+} release lead Ca/Si ratio to decrease because ratio's denominator is greater.
- Ca^{2+} in solution allows precipitation processes analogues to previous experiments (sections 5.2.1 and 5.2.2). All precipitated Ca^{2+} ions as $Ca_3(VO_4)_2$ are translated to a ratio's numerator decrease and, consequently, the ratio as a whole may be lower.
- Once CSH dissolution starts, obtained Ca/Si ratios (by aliquots analyse) fit in values obtained in CSH samples characterisation by SEM (section 5.1.1.4), including the average value Ca/Si=1.19. Actually, it indicates CSH nanoparticles suspension, confirming thus its presence.

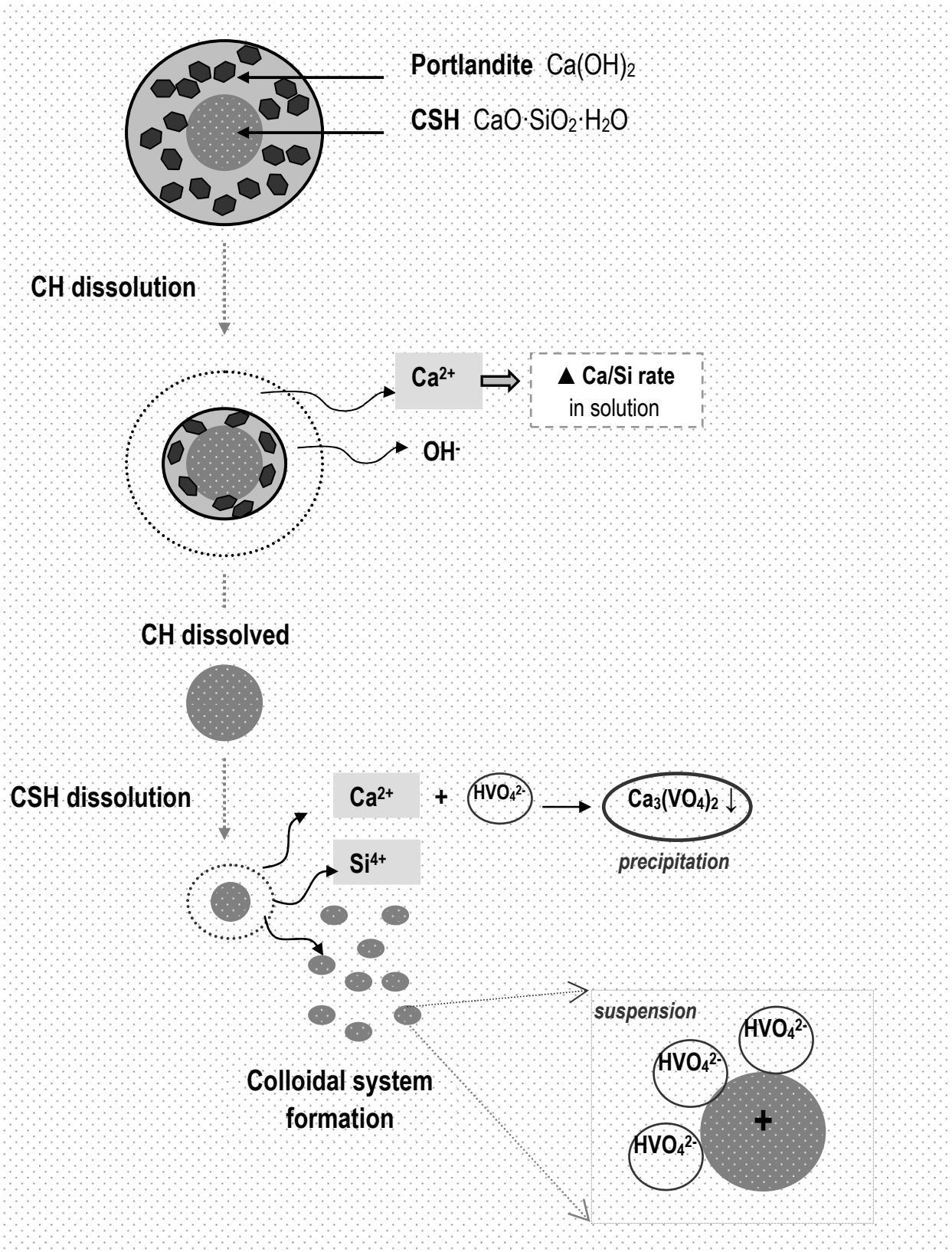

Figure 5.22. Outline of mechanisms related to Ca/Si ratio evolution with CSH as substrate.

Taking into account the surface charges in order to determine the possible cause of this difference, it's important to emphasize that both substrates present remarkable differences concerning to surface charge. Portlandite is known to have no attractive surface charge [Pan et al, 2010], while **CSH denotes a complicated variable surface charge**, changing with the composition and conditions of the solution [Jönsson et al, 2005]. So, retention mechanisms and the interactions of vanadium with cement particles could be controlled by the charge of the surface.

According to charge dispersal model [Yousuf et al, 1995], **CSH should normally present a negative surface charge**, **basing the justification on "Charge Dispersal Model"**. To understand this model it's necessary to introduce the *Zero Potential Charge* (ZPC) concept, corresponding to the pH value at which surface charge is null, considering that superficial charge and the pH of the medium containing the particles are closely linked concepts. Due to extremely basic conditions in cementitious systems, minerals' ZPC will always be lower than cement pastes pH. In other words, the hydrated cement paste is highly alkaline (pH~13±0.5) and in this environment the cement surface (or the newly formed CSH phase) has a negative charge because the ZPC of silicate minerals in the cement system will be always much lower than cement paste pH. Bearing in mind this argument, the sign of the substrate is expected to control the s/s of ionic species:

- **if pH > pH_{zpc} → CSH Negative surface charge → cations adsorbed (X^+)**
- **if pH < pH_{zpc} → CSH Positive surface charge → anions adsorbed (X^-)**

However, considering the results in this study, there's an evident removal of vanadium from the solution, and the explained argument doesn't fit with obtained experimental results. Based on the last conditions, in this study there should be no retention of vanadium oxyanions from the solution because the pH values reached would always be the highest ones in the system and this would be associated to a negative CSH surface charge.

Nevertheless, reasoning changes when considering Ca^{2+} ions as most abundant counter ions in cement solution, originally from portlandite dissolution, extruded from inside the grain through the semi-permeable CSH membrane which acts as a diffusion barrier after the initial period of hydration reaction. Therefore, these oppositely charged Ca^{2+} ions immediately surround the negatively charged CSH surface and preferentially adsorb, due to their higher charge density, giving place to appositively charged layer. Consequently, they both constitute an "Electrical Double Layer" by following the "Charge Dispersal Model" [Yousuf et al, 1995]. Yousuf and co-workers confirm that ions forming the electrical bi-layer must be tightly bounded ("Ca^{2+} bridge" model).

A double layer is a structure appearing on the surface of an object when it is placed into a liquid, and it refers to two parallel layers of charge surrounding the object. The first layer (with either positive or negative surface charge) comprises ions directly adsorbed onto the object due to a host of chemical interactions. The second one (diffuse layer) includes ions attracted to the surface charge [Yousuf et al, 1995].

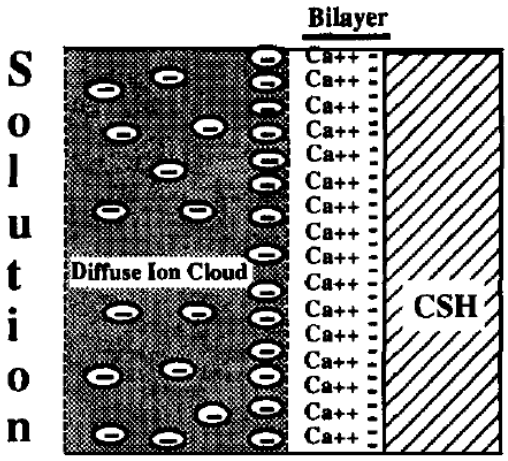

Figure 5.23. Charge dispersal generalised model representation

So, vanadium oxyanions are not expected to adsorb on the negative CSH surface, but the charge-compensated by Ca^{2+} ions will allow the disposal of a "Tri-layer of Diffuse Ions" by adding, according to charges affinity, the next diffusive layer of vanadium oxyanions, as shown in Figure 5.23.

Although the importance of Ca^{2+} ions is considered in all the previous works, "Ca^{2+} bridge" model is not always agreed. It is certainly clear that a good and detailed enough description of CSH surface behaviour in a highly alkaline solution doesn't exist.

Previous studies [Jönsson et al, 2004] have demonstrated consistent trends in the surface chemistry of CSH ($CaO\text{-}SiO_2\text{-}H_2O$) according to OH^-, Ca^{2+} and SiO^{4-} ions, which perfectly fit with experimental results obtained in the present study. The outer surfaces of the CSH nanoparticles are made of silicate, having SiOH surface groups that, at high pH, react with OH^- ions of the solution to give ≡Si–O^- sites (presence of ≡Si-O^- sites is related to the abundance of OH^- ions in the solution and determine the surface charge density) according to Reaction 5.3 [Jönsson et al, 2005]:

$$\equiv SiOH + OH^- \rightarrow \equiv SiO^- + H_2O \qquad \text{(Reaction 5.3)}$$

It leads particles to carry a very negative charge density (δ). This argument is also corroborated by other works [Van Damme and Gmira, 2006]. As far as surface properties are concerned, the CSH layers should bear a mixture of ≡Si–OH and ≡Si–O^- groups. The proportion of the later increases as the Ca/Si ratio as well as the pH increases because of a major presence of OH^-. Thus, CSH nanocolloids are intrinsically negatively charged. However, due to the strong affinity of the Ca^{2+} ions for the ≡Si–O^- groups, charge reversal may occur. This phenomenon only resulting from ion-ion electrostatic correlation is known as *overcharging* by the strong accumulation of couterions in contact with a charged surface [Labbez et al, 2007].

Apparent charge of CSH nanoparticles result from surface charges (≡Si–O^-) plus Ca^{2+} counterions charges accumulated at the surfaces. For a high δ, Jönsson and co-workers' model shows that Ca^{2+} accumulation overcompensates for the surface charges. Therefore, the reversal of apparent particle charge is a consequence of their very high δ and a great of Ca^{2+} ions in the solution (while considering that a great δ means having a high pH. In other words, charge reversal is given by an

interaction between anionic ≡Si–O^- groups (on CSH nanoparticles) as well as the amount $Ca(OH)_2$ added in solution.

So, the proposed behaviour of CSH surface charge is the following:

- **pH <11.6 → ↓δ (≡Si–O^-) and ↓$[Ca(OH)_2]_{dissolved}$→ negatively charged CSH nanoparticles**
- **pH > 11.6 → ↑δ and ↑$[Ca(OH)_2]_{dissolved}$ → positively charged CSH nanoparticles**

Electrophoretic measurements [Van Damme and Gmira, 2006] show that CSH zeta potential increases with the Ca/Si ratio (which is itself determined by the calcium concentration and pH in the solution in equilibrium with the solid). It becomes positive as soon as the Ca/Si ratio is >0.8, indicating that the calcium ions compensating the layer charge are potential-determining [Viallis-Terrasse et al, 2001]. With the highest CSH Ca/Si ratios, the zeta potential ranges from +10 to +20 mV [Van Damme and Gmira, 2006].

The main difference between Jönsson et al. and Yousuf et al. experimental works is that the first one confirms that CSH surface charge reversal does not require a chemical binding of the Ca^{2+} ions (i.e., "Ca^{2+} bridge" model). Taking into account Jönsson's et al work, this overcompensation cannot be explained by bean field models because the surface charge would be only partly compensated by counterions, not strong enough to reverse CSH surface charge. More authors agree that ion-ion correlations, on the basis of pH and Ca^{2+} in solution, can explain a CSH surface sign reversal [Labbez et al, 2007].

Hence, considering CSH surface change reversal for pH>11.5, it can be argued that the positive surface charge will be provided (under the hypothesis above mentioned). Consequently, as indicated in Figure 5.24, vanadium oxyanions can be retained on CSH nanoparticles.

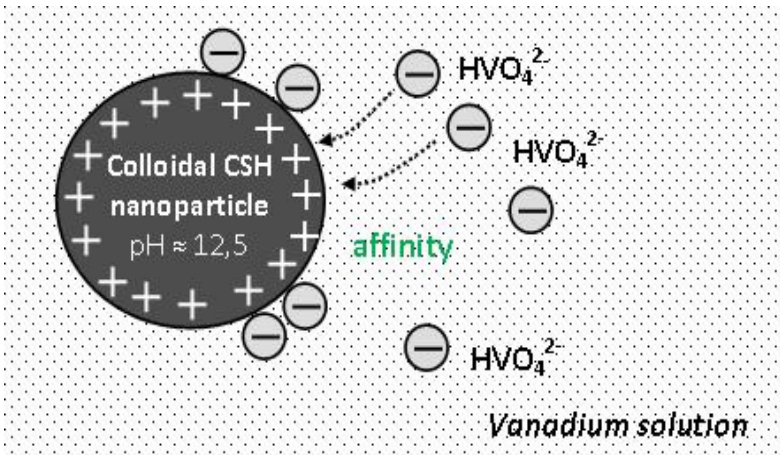

Figure 5.24. Vanadium affinity on CSH surface when pH>11.5.

Colloidal CSH nanoparticles partially remove HVO_4^{2-} oxyanions from the solution. As previously stated, the removal trend on CSH is not the same as on CH and CaO: in CSH experiment, there's a continuous increase of oxyanions removal from the solution but steady state is never reached.

In the case of CH, for example, as vanadium retention mechanisms is precipitation of a solid form, by extracting aliquots from the supernate of the CH experiment (which are subsequently analyzed) no vanadium is not taken because it is no longer in suspension. On the contrary, in CSH experiment, there's no evident solid phase precipitation. CSH colloidal nanoparticles keep on removing HVO_4^{2-} oxyanions, which are in solution, and at the same time they become bigger. Consequently, the area/volume rate decreases, leading to a decrease of the surface area where oxyanions can be retained, being well perceived at 400 min of experimental time. Also having in mind that, before colloids grow enough as to precipitate, they remain in suspension. Therefore, vanadium retention trend on CSH does not completely achieve a clear equilibrium yet: by taking aliquots, CSH colloidal nanoparticles containing vanadium oxyanions are also extracted. Then, these vanadium quantities analysed by ICP from the aliquots are not completely free in suspension (not to be confused with non retained vanadium) but retained in CSH, which it is still suspended until weighting enough.

Results obtained in vanadium retention experiments with CSH are summarized as follows:

I. CSH nanoparticles have a negative surface charge in the experimental conditions

As medium pH≈12-12.6 > pH_{ZPC}=11.6, particles behave as negatively charged. The cause is having a really basic pH that leads to a high OH^- concentration, which surrounds completely and uniformly CSH nanocolloids. The charge reversal leads to the abundance of ≡Si–O^- groups, being responsible of the high surface charge density (δ) in the CSH.

II. As CSH is negatively charged, solution Ca^{2+} counterions are attached to its surface.

Due to extremely basic pH in the solution, portlandite decomposes and releases Ca^{2+} counterions in the solution. These positively charged ions have affinity to the highly opposite CSH surface charge. Therefore, CSH accumulated Ca^{2+} ions increases because of the previously increased δ.

III. CSH surface charge becomes positive due to overcompensation.

If $Ca(OH)_2$ availability is high enough, according to the already cited conditions (negatively charged CSH and high pH, Ca^{2+} and ≡Si–O^- groups), a CSH charge reversal takes place becoming positively charged. This reversal is not related to Ca^{2+} bounds theories (no evidence of its presence is found), while going beyond the dispersion model: it is mostly related to the high CSH δ, which allows an extensive accumulation of Ca^{2+} ions to the extent that surface is overcompensated.

IV. HVO_4^{2-} oxyanions are retained on the positive surface of CSH colloidal nanoparticles, but without being completely removed.

The positive CSH surface charge attracts and captures HVO_4^{2-} from the solution. However, these oxyanions are not completely removed from the solution because CSH nanoparticles keep on growing and precipitate. Therefore, its potential surface area is lower and oxyanions retention decreases with time.

V. Simultaneously, some HVO_4^{2-} oxyanions precipitate next to Ca^{2+} counterions.

High pH promotes a vanadium and calcium salt precipitation ($Ca_3(VO_4)_2$). So, on the one hand, some HVO_4^{2-} are retained on the CSH colloidal nanoparticles (which remain in the solution) and, on the other, the remaining HVO_4^{2-} precipitate as $Ca_3(VO_4)_2$.

VI. Vanadium retention reaches the stabilization phase.

At the same time, CSH colloidal nanoparticles constantly capture HVO_4^{2-} from the solution as well as increasing their volume. When there are no more positive sites in CSH surfaces, the equilibrium is expected to be achieved. In this study, the stabilization phase is not clearly reached but it's intuited just beyond the 500 minutes of the experiment. On the other side, $Ca_3(VO_4)_2$ precipitation is going to stop when no more vanadium is available in the solution (as happens with experiments with portlandite as substrate, but with CSH there are two competing mechanisms for the retention of vanadium).

Accordingly, it's important to highlight that retention percentages from Figure 5.19 correspond to the amount of vanadium either precipitated as a vanadium salt or adhered to CSH nanoparticles that have precipitated due to its weight gain. The remaining vanadium percentages in the solution correspond to oxyanions adhered to colloidal CSH nanoparticles still suspended.

5.2.4. Removal kinetic comparison

Figure 5.25 compares the retention kinetics for commercial portlandite, *insitu* portlandite and CSH.

As observed, and considering previous justifications for each product, the three substrates show different vanadium retention from the solution.

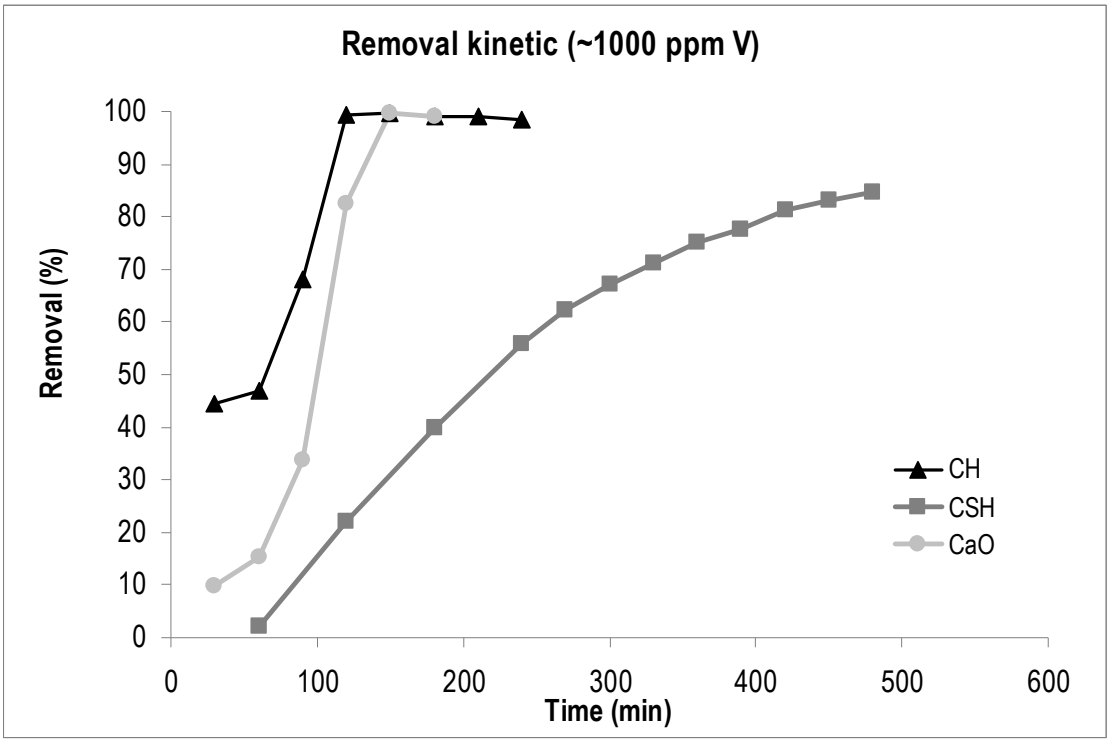

Figure 5.25. Removal kinetic comparison for CSH, *insitu* portlandite and commercial.

- One the one hand, **both portlandites**, the commercial one (CH in Figure 5.25) and CaO that forms *insitu* portlandite (CaO in Figure 5.25), show a completely **similar behaviour**, consisting in a continuously increasing removal from the solution until **reaching the equilibrium** state, meaning that the **100% vanadium is removed**.

- On the other, **CSH behaves** in a **different** way. In fact, contrary to both portlandites, CSH curve trend is **characteristic of adsorption trends** for any substrate, which is identified immediately because all of them show an **increasing tendency** (but with a lower slope than portlandites) followed by a phase where the **slope is decreasing gradually**. Therefore, an exponential curve can be represented, meaning that there's a continuous and increasing removal of vanadium but, later, removal kinetics slows down preventing the achievement of the equilibrium state in the system, meaning that vanadium is not removed completely. There's a partial removal on CSH system, which is explained through the mechanisms detailed previously. Considering previous research studies [Cornelis et al, 2008], CSH includes disordered layers that create a large volume of micropores and a vast specific surface area, available for sorption. Therefore, when positively charged, CSH can exhibit an adsorption potential for arsenate, arsenite, selenite and to a limited extent also chromate. In addition, taking into account obtained results related to HVO_4^{2-} oxyanions retention on CSH, it can be stated that such vanadium oxyanions can also be adsorbed in CSH. In this way, the present work contributes on research field about oxyanions retention in cementitious materials, especially in determining the mechanisms by which vanadate oxyanions can be retained in such materials.